INTERNATIONAL JOURNAL OF ENERGY STUDIES

e-ISSN: 2717-7513 (ONLINE); homepage: https://dergipark.org.tr/en/pub/ijes

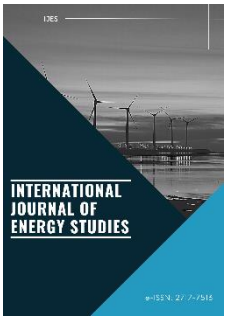

Review Article

Int J Energy Studies 2023; 8(4): 879-898

DOI: 10.58559/ijes.1356955

Received : 08 Sep 2023

Revised : 05 Nov 2023

Accepted : 05 Nov 2023

Comparative performance analysis of NACA 2414 and NACA 6409 airfoils for horizontal axis small wind turbine

Abdullah Tokul[a*], Ünal Kurt[b]

[a] *Graduate School of Natural and Applied Science, Amasya University, Türkiye, ORCID: 0000-0003-0479-4867*

[b] *Graduate School of Natural and Applied Science, Amasya University, Türkiye, ORCID: 0000-0002-8889-8681*

*(*Corresponding Author: abdullah.tokul@amasya.edu.tr)*

Highlights

- Performance measurement of NACA 2414 and NACA 6409 series airfoils in the range of $1x10^6$ constant Reynolds number and 0-20^0 attack angles.
- Comparison of different features such as lift (C_l) and drag (C_d) coefficients, pressure distribution on the wings, power coefficients with Q-Blade software.
- Analyzes were made using a calculation method based on Blade Element Momentum (BEM) theory.
- Comparative analysis of moment, torque, thrust and power coefficient based on tip speed ratios for both airfoils.

You can cite this article as: Tokul A, Kurt Ü. Comparative performance analysis of NACA 2414 and NACA 6409 airfoils for horizontal axis small wind turbine. Int J Energy Studies 2023; 8(4): 879-898.

ABSTRACT

While wind energy, which has an important place among renewable energy sources, is converted into electrical energy by means of wind turbines, the designs and aerodynamic behaviors of turbine blades gain importance in order to obtain optimal efficiency. The most important factor affecting the wind energy capture performance and aerodynamic behavior of the blade is the airfoil structure. In this study, the design and comparative performance analysis of NACA 2414 and NACA 6409 series airfoils under wind turbine conditions with $1x10^6$ fixed Reynolds number, 0-20^0 attack angles, constant air density and ambient conditions, 3kW nominal power and 2m blade length were carried out. The designs and analyzes for both airfoils were simulated using Q-Blade software version 2.0.5.2. While designing the blade, the propeller blade was divided into 20 equal parts so that there would be no aerodynamic interaction between the elements, and analyzes were made with a calculation method based on the Blade Element Momentum (BEM) theory. As a result, by comparing different features such as lift (C_l) and drag (C_d) coefficients, pressure distribution on the blades, power coefficients, it was seen that the NACA 6409 airfoil was more efficient than the NACA 2414 airfoil for small diameter wind turbines.

Keywords: Horizontal axis wind turbine, Q-Blade, NACA 2414, NACA 6409, Blade element momentum, Airfoil, Lift coefficient, Drag coefficient

1. INTRODUCTION

The sun's rays reaching the earth create different temperatures in different parts of the world, causing air movement from high-pressure areas to low-pressure areas and creating wind energy. About 2% of the 145 million GWh energy that the world receives from the sun can be converted into wind energy, and according to the data of the Turkey Wind Energy Potential Atlas (REPA-V1), it has been determined that the total capacity of wind power plants that can be established in our country in areas with a height of fifty meters above the ground and an annual average wind speed of over 7.5 m/s is 48 GW [1]. In order to optimally evaluate the electrical energy potential that can be produced from wind energy by wind turbines in a region, the efficiency of the turbines to be established must be high. Wind turbines consist of four main elements: tower, blades, generator and mechatronic connection elements. The energy losses that will occur in each of these equipment will adversely affect the turbine performance. Therefore, the blade structures of the wind turbine are an important factor affecting the efficiency and the blade efficiency is largely determined by the structure of the blade profile [2]. Academic studies on the airfoil show that choosing the ideal blade section increases the amount of energy produced by the wind turbine and reduces the unit cost [3].

The lift and drag coefficients of the wing determine the wind turbine blade performance, and in order for the aerodynamic performance to be high, the lift coefficient (C_l) of the airfoil profile should be as high as possible and the drag coefficient (C_d) should be as low as possible [4]. While many academic studies have been carried out on the aerodynamic performance of airfoils, some developments have been made regarding the NACA 2414 and NACA 6409 airfoils, which are particularly emphasized in this study. In his examination, Zahari [5] examined 10 NACA airfoils of different designs, including NACA 6409. In the same conditions, airfoils with the highest C_d value from the lowest drag coefficient (C_d) value, concluded that the NACA 0006, NACA 1408, NACA 2408, NACA 0009, NACA 1410, NACA 0015, NACA 6409, NACA 2418, NACA 6412, and NACA 4424, respectively. Hossain, Raiyan, Akanda and Jony [6], performed aerodynamic performance analysis for NACA 6409 and NACA 4412 airfoils using Ansys Workbench 14.5 software, using finite element method and computational operations dynamics run, and meeting the results such as drag and lift coefficients, pressure drop on the wings, NACA 4412 found airfoil to be more efficient than NACA 6409 airfoil.

Kumar, Jhawar and Kalraiya [7], created a NACA 6409 airfoil using the computational fluid dynamics (CFD) method with Ansys 14.0 software and performed a low Reynolds number(Re) and lift and drag coefficient analysis at a constant wind speed of 4m/s, angles of attack between 1^0 and 15^0. As a result, he observed that the C_l/C_d ratio of the airfoil increased in the range of 1^0 to 6^0 angle of attack, peaked at 6^0 at about 65, and decreased again in the range of 6^0 to 15^0 angle of attack. Tarhan and Yılmaz [8], in the comparative aerodynamic performance analysis of 14 different blade profiles for small diameter wind turbines according to Kayseri conditions, using Ansys Fluent software with 50,000 Re in the range of 0^0 to 15^0 attack angles, the efficiency ranking from largest to smallest is BW3, A18, SD7032, S7012, E387, RG15, Clark Y, S6062, SD6060, SD7062, NACA2414, S822, S823, FX77. Oliveira and Cândido [9], for 3-blade horizontal axis small scale wind turbines, NACA series 0012, 1412, 6409 profiles, keeping other conditions constant, they investigated the actuation times in the 1m/s - 5m/s wind speed range and according to 15°, 30° and 45° inclination angles. The NACA 6409 airfoil starts to rotate at a wind speed of 1.6 m/s at 45°, 1.6 m/s at 30° and 2.0 m/s at 15°, respectively, according to the tilt (pitch) angles, for the NACA 0012 airfoil, it starts to rotate at a wind speed of 1.6 m/s at 45°, 1.6 m/s at 30° and 1.3 m/s at 15°, finally, NACA observed that the 1412 airfoil began to rotate at a wind speed of 1.2 m/s at 45°, 1.3 m/s at 30°, and 1.0 m/s at 15°. Therefore, it has been determined that NACA 1412 is better than NACA 0012 and both are more efficient than NACA 6409 in terms of take-off performance. Sandanshiv and Chavan [10], investigated the C_l, C_d, C_l/C_d ratio and angles of attack of NACA 2414, NACA 0024, NACA 0012 and NACA 2424 airfoils using the blade element momentum method, observed that the output power obtained under the same conditions, that is, aerodynamic performance, is in the order of NACA 0012, NACA 2414, NACA 2424 and NACA 0024. Muftah [11], in his study on the NACA2414 airfoil model, investigated the lift coefficient (C_l), drag coefficient (C_d) and C_l/C_d ratio at varying angle of attack and Re, it was concluded that the C_l/C_d ratio increased with the increase of the Re and the maximum aerodynamic efficiency was obtained at the angle of attack at 5°. Madhavan [12], in his study in which he analyzed the change in aerodynamic performance by adding a gurney wing at a height of 6% of the chord length to the NACA 2414 airfoil, proved that the airfoil of the gurney wing had a positive contribution to the lift/drag coefficient ratio. Islam, Bashar, Saha and Rafi [13], NACA series 2412, 2415, 2418, 4412, 4415, 63(2)-615, 6409 blade profiles in $1x10^5$ and $3x10^5$ Re between $0^0 – 15^0$ angles of attack with Q-Blade software and aerodynamic performance analyzes of NREL series S817, S821, S822, S823, S825, S834 and S835 airfoils were made and for both Reynolds values, 6409 in NACA series, it is stated that S825 is more efficient in the NREL series, and in the general evaluation,

NREL airfoils are more suitable than NACA airfoils due to stability criteria. Kulshreshtha, Gupta and Singhal [14], compared the lift and drag coefficients of NACA 2412, NACA 2414 and NACA 2415 airfoils in the range of -5^0 to 20^0 attack angles and constant air speed conditions using computational fluid dynamics method. As a result of the comparison, in terms of C_l/C_d ratios, NACA 2412 is in the first place with 27.92, NACA 2415 is in the second place with 26.32, and NACA 2414 is in the third place with 23,56.

Mankotia, Channi and Gupta [15], analyzed E387, S1223, SD7080, NACA2414 blade profiles for a 2kW wind turbine, respectively, with low Re using Q-Blade software and found the maximum lift/drag coefficient ratios at 7, 7, 3, 5 angles of attack, respectively, as 70, 60, 59.2, 54.2 in the same order. Hwas and Hatab [16], examined the power performance, lift (C_l), drag (C_d) coefficients and thus the design parameters affecting the power (C_P) coefficient for small scale horizontal axis 3-blade wind turbines using the Taguchi method. It was determined that the most influential design parameter on the airfoil coefficients was the Re with 72.6% contribution, followed by the angle of attack with 16.8%, the interaction with 9.1% and the airfoil with 1.5%. Gray, Singh and Singh [17], using Q-Blade software for airfoil design and X-Foil analysis, has designed a new special airfoil named G4510 to increase the aerodynamic performance of wind turbines for low speed regions and has a wind speed range of 2-6m/s and percolation ratio (C_l/C_d) analyzes were performed at $3x10^4$, $6x10^4$, $9x10^4$ Re. As a result, they observed that the efficiency of the G4510 airfoil was 52.2% higher than NACA 2412 for Reynolds $3x10^4$, 21.92% higher than NACA 4412 for $6x10^4$ and 3.24% higher than NACA 6409 for $9x10^4$. Kulshreshtha, Goyal and Singh [18], used Ansys Fluent 15.0 software to analyze the comparative flow behavior of NACA 2412, NACA 2414 and NACA 2415 airfoils, 4 different turbulence models, namely standard k-ε, standard k-ω, Reynolds stress model and transitional k-kl-ω models, were used and the k-epsilon model in the 5° to 20° angle of attack range, it has been found that it provides more efficiency than other models.

Solanki [19], carried out aerodynamic performance analysis at 0^0-15^0 angle of attack and wind speeds of 4m/s, 5m/s, 6m/s by using the computational fluid dynamics method with Ansys CFX software, taking the NACA 6409 airfoil as a reference. He concluded that the C_l/C_d ratio peaked at 5^0 attack angles at 4m/s and 5m/s wind speeds, and at 4^0 angles of attack at 6m/s wind speeds. Ahammed [20], using Ansys Workbench 2020 R1 software, to find the effect of angle of attack towards the floating horizontal axis wind turbine blade and to obtain the best blade performance

between the twisted and non-untwisted blades to give the maximum lift and drag coefficient. performed the analysis, concluded that the aerodynamic performance of the twisted blade wind turbine is more efficient than the straight blade wind turbine. Widyalankara, Jayawickrama, Ambegoda and Velmanickam [21], simulated an energy storage wind farm that converts the wind energy from the wind of the vehicles into electrical energy for the roadsides with MATLAB Simulink software and performed the performance analysis. Researchers who prefer vertical axis wind turbines in the power plant design, with Q-Blade software, NACA series 0012, 2412, 2415, 2418, 4412, 4415 and 6409 blade profiles, by performing a comparative performance analysis at $1x10^5$ Re, they determined that the most efficient airfoil in the 0^0-20^0 angle of attack range was NACA 6409 and included it in the facility design.

2. MATERIAL AND METHOD

In the study, the design and comparative performance analysis of NACA 2414 and NACA 6409 series airfoils were carried out with a calculation method based on wing element momentum (BEM) theory using Q-Blade software. As environmental conditions, a constant Re of $1x10^6$, constant air density in the range of attack angles of 0-20^0 were preferred. A turbine model with 3kW nominal power and 2m blade length was adopted as the wind turbine structure. In this section, the wind turbine blade design parameters and analysis materials mentioned in the study are explained.

2.1. Q-Blade Software and Blade Element Momentum Theory

Q-Blade software was developed in 2010 at the Faculty of Mechanical Engineering and Transport Systems at the Technical University of Berlin, Dr.-Ing. Developed by a research team led by David Marten, it is a C++ based free license software [22]. It facilitates processes such as designing the airfoils needed for aero-servo-hydro-elastic simulation of horizontal or vertical axis wind turbines, simulating performance analyzes and integrating the obtained data into a wind turbine rotor design [23]. The software author carried out a doctoral study in 2020 presenting the methods applied in Q-Blade simulation and explaining the logic of choosing and classifying among different simulation methods that can be applied to model wind turbine blade profiles [24]. Blade Element Momentum (BEM) theory is one of the oldest and most common methods used in Q-Blade software to calculate induced speeds in wind turbine blades and to determine the properties of blade profiles. This theory is a refinement of the actuator disc theory proposed by the pioneering

propeller work of Rankine and Froude in 1878 and consists of a combination of 'blade element theory' and 'momentum theory' [25].

Blade element theory, assumes that blades can be subdivided into small aerodynamically operating elements in the form of two-dimensional airfoils, which act independently of the surrounding elements and whose aerodynamic force components can be calculated according to local flow conditions. Axial and thrust forces applied to these small elements formed are summed along the wingspan, so that the total force and moments applied on the turbine are calculated. With this approach, the axial (F) and thrust (T) forces are respectively expressed as:

$$dF = \frac{1}{2}.\rho.B.d.W^2.dr[C_l cos\emptyset + C_d sin\emptyset] \quad (1)$$

$$dT = \frac{1}{2}.\rho.B.d.W^2.r.dr[C_l sin\emptyset - C_d cos\emptyset] \quad (2)$$

In these equations, air density ρ, number of blades B, airfoil chord length d, resultant velocity W, distance of the element from the hub (connection center) r, lift coefficient C_l, drag coefficient C_d, and flow angle ∅ correspond to expressions [26].

Momentum theory, the other half of the BEM, assumes that the pressure or momentum loss in the rotor plane is due to the work done on the blade elements by the airflow passing through the rotor plane. Using momentum theory, induced velocities can be calculated from the momentum lost in flow in the axial and tangential directions. With this theory, assuming that the blades can generate power without rotational motion, the axial force is expressed as:

$$dF = 4.a.(1-a).\rho.V^2.\pi.r.dr \quad (3)$$

When rotation is added to the model, the thrust (T) force is expressed as:

$$dT = 4.a'.(1-a).\rho.V.\Omega.\pi.r^3.dr \quad (4)$$

Here, the axial induction factor a is expressed as:

$$a = \frac{V - V_T}{V} \tag{5}$$

a' is the angular induction factor expressed as:

$$a' = \frac{\omega}{2\Omega} \tag{6}$$

It is expressed in the equations using the downwind speed V, the upwind wind speed V_T, the blade rotation speed ω and the angular velocity Ω. The combination of the two theories creates the blade element momentum theory (BEM) and establishes a repeatable process for calculating aerodynamic forces and induced velocities around the rotor. For this, the equations obtained from momentum theory and blade element theory are combined;

$$8.a.(1-a).V^2.\pi.r = B.d.W^2.[C_l cos\emptyset + C_d sin\emptyset] \tag{7}$$

$$8.a'.(1-a).\rho.V.\Omega.\pi.r^3 = B.d.W^2.[C_l sin\emptyset - C_d cos\emptyset] \tag{8}$$

Two important equations of BEM are obtained [25].

2.2. Aerodynamic Analysis Parameters

Airflow striking the blades of a wind turbine is split at the leading edge of the blade, passing over and under the blade at different speeds and ending at the trailing edge. The forces created by the air flow on the wing were explained in 1738 by the Swiss mathematician Daniel Bernoulli. According to Bernoulli's principle, the air pressure on the wing decreases due to the acceleration and stretching of the air flowing from the upper surface of the wing. In contrast, the air flowing under the wing moves in a straighter line, so its velocity and pressure remain approximately the same. Bernoulli's equation is used to express the pressure changes of the flowing air and the equation is as follows;

$$P + \frac{1}{2}.\rho.V^2 = constant \tag{9}$$

Here P is pressure, ρ is air density, V is wind speed [27].

Due to the effect of air flow, low pressure occurs on the upper surface of the wing and high pressure on the lower surface. Since the air movement will occur from high pressure to low pressure, it creates **lift force** on the wings. As the pressure difference between the upper surface and the lower surface of the wing increases, the lift force increases in direct proportion. The lifting force is expressed by the following equation;

$$L = \frac{1}{2}.C_l.\rho.A.V^2 \tag{10}$$

With the movement of the turbine blades, a second force occurs in the direction of the movement and in the opposite direction of the movement, and this force is called the **drag force**. This force can also be called the resistance force against the air flow. The drag force is expressed by the following equation;

$$D = \frac{1}{2}.C_d\ .\rho.A.V^2 \tag{11}$$

The ratio of the blade's lift and drag coefficients determines the wind turbine blade performance, and the angle with the highest lift force and the least drag force is the angle with the highest blade performance. This angle is considered the design angle in wind turbines [28]. One of the most important coefficients used in fluid mechanics is the Re and is used to characterize different flow regimes such as laminar flow and turbulent flow. Reynolds number (R_e), a dimensionless number defined by Osborne Reynolds in 1883, is expressed as the ratio of the inertia force (ρV) of the fluid to the viscosity force (μ/d).

$$R_e = \frac{\rho.V.d}{\mu} \tag{12}$$

Where, V is the speed of the air, μ is the dynamic viscosity of the air, ρ is the density of the air, and d is the blade chord length [29]. For the airfoils sampled in the study, since the separation event will be later at high Re values, it will have a positive contribution to the Cl/Cd ratio, and the flow model in the range of 50,000-1,000,000 Re is called Re with low aerodynamics [30]. One of the parameters defined when performing airfoil analysis with the Q-Blade is the Mach number. This number, named after the Austrian physicist Ernst Mach, is expressed as the ratio of the speed

of the wind hitting the turbine blade to the speed of sound in its environment. At sea level, at an air temperature of 15°C and a pressure of 1 atm, 1 Mach=340 m/s is specified, and as you go higher, the air temperature also decreases, accordingly the speed of sound slows down. For this reason, for the same speed value, the Mach number of a mass at high altitude is higher than the Mach number it has at sea level. Mach number is calculated by equation 13.

$$M = \frac{V_\infty}{a_\infty} \tag{13}$$

Subsonic, transonic and supersonic air currents can flow on the turbine blade profile. Subsonic (subsonic) for currents below Mach 0,8 or 273 m/s from these airflow regimes, transonic for air currents in the range of 0,8 to 1,2 Mach or 273-409 m/s, air currents in the range of 1,2 to 5 Mach or 410-1702 m/sec are classified as Supersonic [31]. The **N-Crit coefficient**, short for critical amplification factor, essentially determines the sensitivity of the flow to disturbances. A higher N-Crit value represents more laminar flow, while a lower N-Crit value represents more turbulent flow. The high N-Crit coefficient minimizes distortion by maximizing the extension of laminar flow under specified wind speed and ambient conditions. Under low N-Crit conditions, a large amount of turbulent flow is assumed to increase the surface frictional resistance. Q-Blade software performs the simulations of these uncertainty coefficients with the e^N method and can define the highest N-Crit coefficient as 9 (min. distortion) and the lowest N-Crit coefficient (max. distortion) as 0 [32]. The ratio of the tangential speed of the blade tip to the speed of the oncoming wind, expressed as the **tip speed ratio** (TSR), is a factor that explains how densely packed the vortex rings are behind the turbine [24].

Some passive control methods are used to accelerate the transition of the laminar flow on the airfoil to turbulence on the trailing edge, thus accelerating the recovery from the unstable situation in the air flow [39, 36]. These are generally applications such as vortex generators applied to the wing surface, some geometric changes, materials that create roughness on the surface, and flexible wing structure. Vortex generators placed before the separation point provide resistance to adverse pressure gradients by adding momentum to the flow and ensure that the flow separation occurs later and closer to the trailing.

Zhu and colleagues performed a numerical analysis on the DU97-W-300 airfoil to evaluate the effect of vortex generators on the unstable airfoil performance and observed that the lift hysteresis intensity was significantly reduced by 60-80% and the lift coefficient increased [40]. In their study examining the effect of Widyawati and Permatasari vortex generators on the aerodynamic structure on the NACA 632-415 airfoil, vortex generators increased the C_l value by 24.9%, the C_d value by 2.7% and the C_l / C_d coefficient ratio by 9.1% [41].

Since 3-bladed propeller models are commonly used in horizontal axis wind turbines, the tip-to-speed ratio should be approximately in the range of 5-8 [33]. The tip speed ratio is expressed with the symbol λ and its formula is presented in equation 14.

$$\lambda = \frac{V_{tip}}{V_{wind}} = \frac{\omega . r}{V_{wind}} \quad (14)$$

In this equation, blade angular velocity ω is expressed as wind speed V and blade radius r [4].

One of the important parameters that determine how efficiently the turbine blade can benefit from the wind power in its environment is the **power coefficient**. The ratio of the wind power gained by the blades to the total wind power in the environment determines the power coefficient. The power factor can be calculated with the equation 15.

$$C_P = \frac{N_K}{N} = \frac{N_K}{0.5\rho\pi r^2 V^3} \quad (15)$$

Here, the power coefficient C_P is expressed as the wind speed V (m/s), the density of the air ρ (kg/m^3), the blade radius r (m) and the power N_K obtained by the blades from the wind [34].

2.3. Blade Airfoil Structure

Thousands of different airfoils have been designed for aircraft and wind turbines, but the most widely used today are the NACA (*National Advisory Committee for Aeronautics*) series of airfoils [35]. NACA airfoils can be classified in six different groups as 4-digit, 5-digit, 1 series, 6 series, 7 series and 8 series. In the study, two different models of 4-digit NACA series airfoils were compared. The 4-step NACA series airfoils were first developed by Eastman N. Jacobs in 1929. NACA defines airfoils according to a specific thickness distribution and mean line. For example,

the maximum camber ratio of the NACA 6409 airfoil is 6%, the ratio of the distance from the maximum camber point to the leading edge to the length of the blade is 40%, and the ratio of the maximum thickness of the airfoil to the length of the blade is 9% [36]. The physical properties of an airfoil are characterized by reference to the NACA 6409 airfoil in Figure 1.

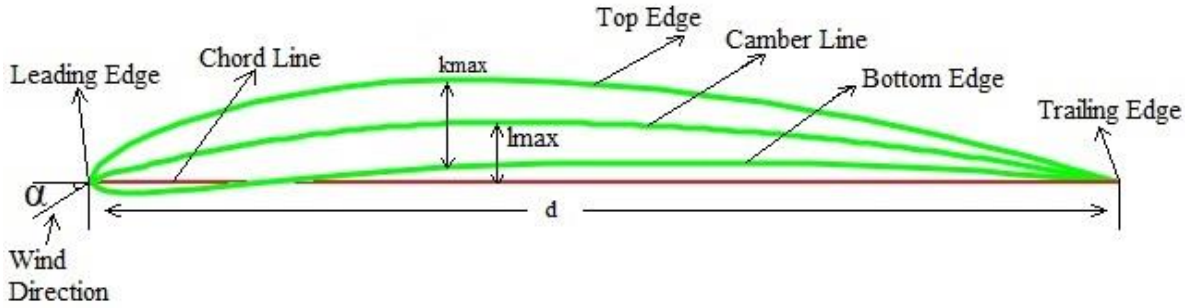

Figure 1. NACA 6409 Airfoil Structure

The wind turbine blade profile consists of two curves, the upper edge and the lower edge, with a general definition. The length between the leading edge where the blade profile receives the air flow and the trailing edge where the flow leaves the profile is called the chord and is denoted by "d". The angle that the wind vectors make with the chord line (beam) is called the angle of attack and is denoted by "α". The curve connecting the leading edge and trailing edge, passing through the middle of the upper and lower edges of the blade profile, is called the camber line. The distance between the camber line and the chord line is called the camber of the blade and "lmax" refers to the point where the camber is maximum. The vertical length between the lower and upper edges of the blade profile is called the blade section thickness and the point where the section thickness is maximum is indicated by "kmax". With reference to Figure 1, the camber ratio representing "a" in the "NACA abcc" structure is calculated with the equation 16.

$$\gamma = \frac{l_{max}}{d} \tag{16}$$

Likewise, the thickness ratio representing "c" in the "NACA abcc" structure can be calculated with the equation 17.

$$\delta = \frac{k_{max}}{d} \tag{17}$$

Airfoils with a thickness ratio below 10% are classified as thin, profiles in the range of 10-14% as medium, and profiles with a ratio above 14% are classified as thick airfoils [28].

2.4. Design and Analysis

In the study, NACA 6409 airfoil, which can be called thin in terms of thickness ratio, and NACA 2414 airfoil with medium thickness ratio were preferred in order to examine their aerodynamic and energy production performances that they will show under the same environmental conditions, and "dat" extension coordinate files were obtained by using the online airfoil generator [37]. After entering the coordinate files into the Q-Blade software, as seen in Figure 2, the basic information of the blade profiles such as thickness ratios, maximum thickness points, camber ratios, maximum thickness points, and total reference point numbers are presented in the "Airfoil Design Module" tab.

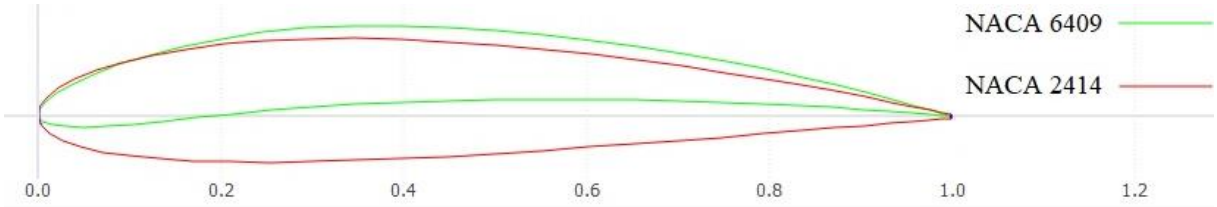

Airfoil Design Module

	Foil Name	Thickness (%)	at (%)	Camber (%)	at (%)	Points	Style
1	NACA6409 9%	9.03	29.30	6.00	39.60	61	
2	NACA 2414	14.00	29.50	2.00	39.60	61	

Figure 2. Q-Blade design image of NACA 6409 and NACA 2414 blade profiles

Although the thickness ratio and camber ratios of both blade profiles are different, it is seen that the maximum thickness points are very close to each other, such as 29.3% and 29.5%, and the maximum camber points are in the same positions with 39.6%. In the second stage, "Airfoil Analysis Module", the basic analysis conditions are determined and the Re is considered to be the starting value of the middle level, with the same value for both airfoil profiles, "$1x10^6$", the Mach number was determined as "0", which is the subsonic environment value, and the N-Crit coefficient was determined as "9" with the minimum surface roughness value. As the angle of attack range where the analysis will take place, the angle range of 0^0-20^0 was preferred with 1^0 sampling steps.

The "HAWT Blade Design" tab was used to design the horizontal axis wind turbine blades, 20 pieces of equal length of 10cm and the same beam dimensions for both blade profiles were used to analyze with the blade element momentum method (BEM) as presented in Figure 3. owner, only the blade design has been made where the NACA 2414 airfoil appears to make 1^0 more twist angles. Figure 4 presents the 3D simulation of the airfoil with a swept area of 12.94 m^2, designed with Q-Blade. Additionally, Betz limit was applied to analyze the energy production performance of the wind turbine. The Betz limit accepts that wind turbines theoretically reach the highest energy production efficiency with a rate of 59.3% [38].

	Part No:	1	2	3	4	5	6	7	8	9	10	11	12	13	14	15	16	17	18	19	20	21
NACA 6409	Location(m)	0,000	0,100	0,200	0,300	0,400	0,500	0,600	0,700	0,800	0,900	1,000	1,100	1,200	1,300	1,400	1,500	1,600	1,700	1,800	1,900	2,000
	Chord(m)	0,030	0,030	0,109	0,099	0,090	0,082	0,075	0,068	0,062	0,056	0,051	0,049	0,044	0,040	0,036	0,033	0,030	0,027	0,025	0,023	0,020
	Twist(Degree)	75,180	50,083	29,050	19,364	13,209	9,041	6,060	3,834	2,112	0,744	-0,369	-1,291	-2,067	-2,729	-3,300	-3,798	-4,236	-4,623	-4,969	-5,280	-5,560
NACA 2414	Location(m)	0,000	0,100	0,200	0,300	0,400	0,500	0,600	0,700	0,800	0,900	1,000	1,100	1,200	1,300	1,400	1,500	1,600	1,700	1,800	1,900	2,000
	Chord(m)	0,030	0,030	0,109	0,099	0,090	0,082	0,075	0,068	0,062	0,056	0,051	0,049	0,044	0,040	0,036	0,033	0,030	0,027	0,025	0,023	0,020
	Twist(Degree)	76,180	51,083	30,050	20,364	14,209	10,041	7,060	4,834	3,112	1,744	0,631	-0,291	-1,067	-1,729	-2,300	-2,798	-3,236	-3,623	-3,969	-4,280	-4,560

Figure 3. Element structure of NACA 6409 and NACA 2414 airfoils

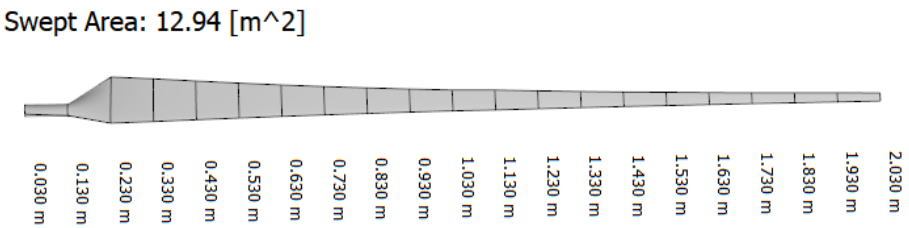

Figure 4. 3D view of NACA 6409 and NACA 2414 blade profiles with 2m length and 0.03m hub connection diameter

As BEM parameters, constant for both airfoils, wind speed is 10 m/s, pitch angle is 0^0, air density is 1,225 kg/m^3, kinematic viscosity is $1{,}647x10^{-5}$ m^2/s, maximum number of iterations is 1000 and the tip speed ratio (TSR) was between 2-12 and the simulation design was carried out with the number of steps (Δ) of 0,2.

3. FINDINGS AND DISCUSSION

The changes in lift, drag, glide and moment coefficients of NACA 6409 and NACA 2414 airfoils in the range of 0^0-20^0 attack angles were observed with the first-stage analyzes using the airfoil analysis module in the Q-Blade software.

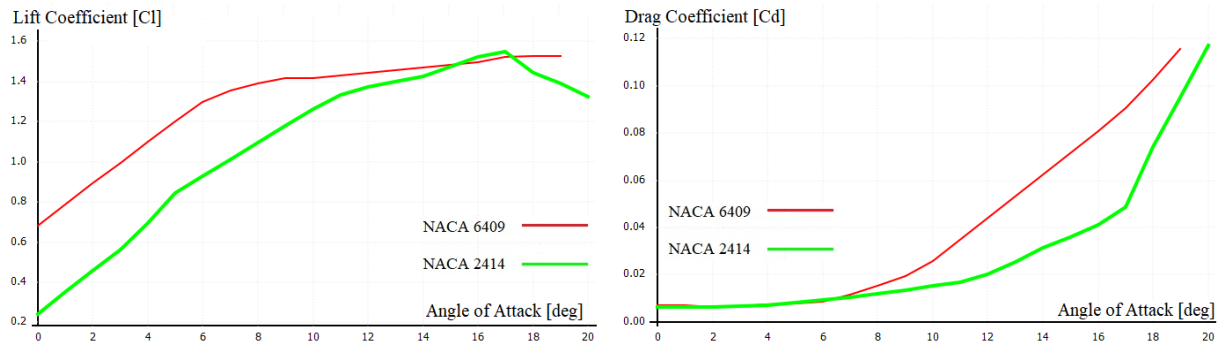

Figure 5. Comparative variation graph of lift(C_l) and drag(C_d) coefficients of NACA 6409 and NACA 2414 airfoils according to angle of attack

According to the lift and drag coefficient change graphs according to the angle of attack presented in Figure 5, the NACA 6409 airfoil is more advantageous in terms of lift at the first 15^0 angle of attack, and NACA 2414 peaking at 17^0 angle of attack, reaching a higher value than NACA 6409, but then decreasing rapidly, on the other hand, it is seen that NACA 6409 continues by increasing its lift coefficient. In terms of drag coefficient, it is determined that both airfoils have the same performance up to the angle of attack of about 7^0, but the drag coefficient of NACA 6409 increases rapidly in the range of 7^0-20^0, while NACA 2414 rises more slowly.

A stall occurs when the angle of attack of an airfoil exceeds the value that creates maximum lift on the airfoil. At the angle of stall, the airflow ceases to make regular contact with the upper surface of the wing and becomes turbulent, greatly reducing lift. In the analysis, it is seen that the stall angle of both airfoils is 17 degrees, as presented in Figure 5.

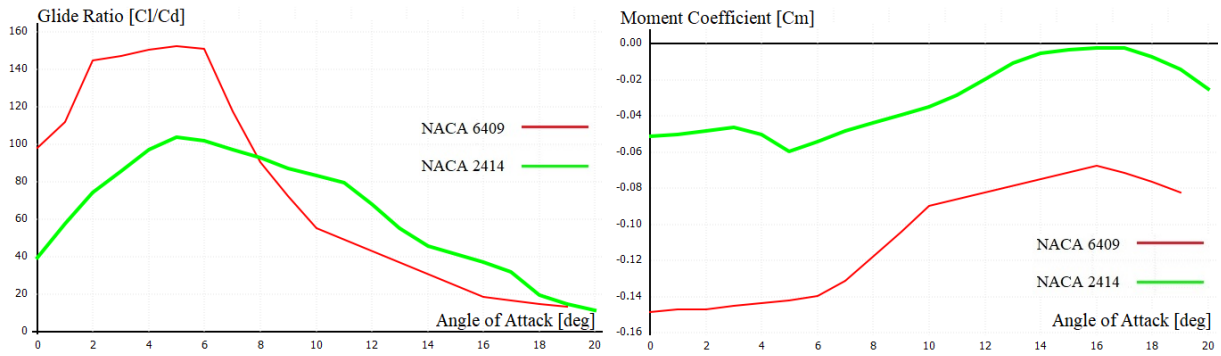

Figure 6. Comparative variation graph of glide(C_l/C_d) and moment(C_m) coefficients of NACA 6409 and NACA 2414 airfoils according to angle of attack

When the glide coefficients of the blade profiles are examined according to the angles of attack, it is seen that both glide profiles reach their peak values at 5^0 angles of attack, as shown in Figure 6, but NACA 6409 has much higher efficiency than the glide coefficient of 152,4 and NACA 2414, which is 104. Although the glide coefficient (C_l/C_d) of NACA 6409 in the 8^0-20^0 angle of attack range is lower than NACA 2414, the high coefficient difference of NACA 6409 in the 0^0-8^0 angle of attack range due to their close values, reveals that NACA 6409 is more advantageous in the overall evaluation. We know that moment is a vector quantity that determines the effect of moving an object along an axis as a result of a force applied to it. In this direction, when the moment coefficients change graph of both airfoils according to the angles of attack presented in Figure 6 is examined, it is seen that the moment coefficient of NACA 6409 is significantly lower than that of NACA 2414.

As a second stage analysis, as a result of Q-Blade "Steady BEM" module analyzes performed with the blade element momentum (BEM) method, power coefficient, thrust coefficient, torque coefficient and generated power amount change graphs are obtained according to tip speed ratios (TSR). We know that torque has the effect of rotating the object about an axis as a result of the force applied to the object. When the torque coefficients of the airfoils are examined according to the tip speed ratios presented in Figure 7, it is determined that NACA 2414 reaches a maximum torque coefficient of $4{,}520 \times 10^{-2}$ at 8,6 TSR, and NACA 6409 reaches a maximum torque coefficient of $4{,}683 \times 10^{-2}$ at 9,4 TSR. Likewise, when the amount of power produced by the airfoils is examined, it is observed that NACA 2414 reaches a maximum power generation of 3,635 kW at 11,8 TSR, and NACA 6409 reaches 3,685 kW at 10.4 TSR.

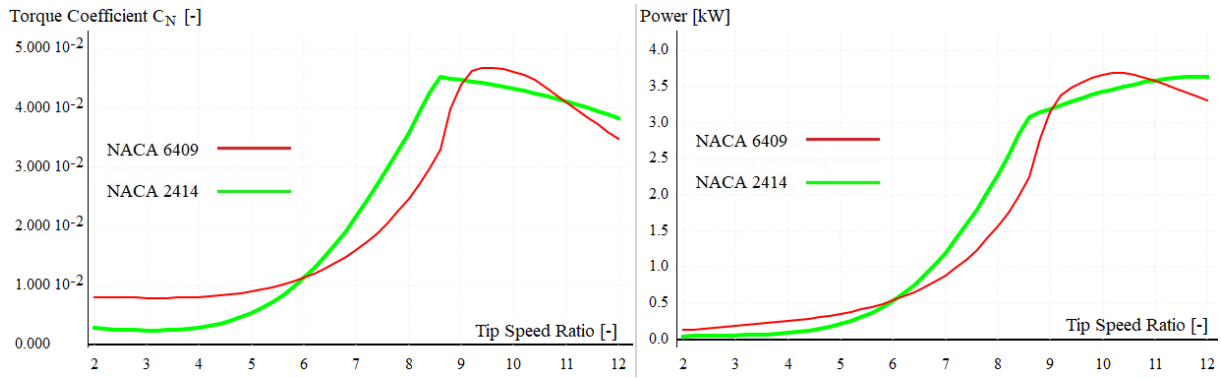

Figure 7. Comparative graph of the torque (C_N) coefficient and the amount of power (kW) they produce according to the tip speed ratios of NACA 6409 and NACA 2414 airfoils

The thrust force is the thrust force acting on the blades and rotor disc with the effect of the wind force. When the change graph of the thrust coefficient according to the tip velocity ratio presented in Figure 8 is examined, it is seen that the thrust coefficient of NACA 6409 increased much faster after 8,72 TSR.

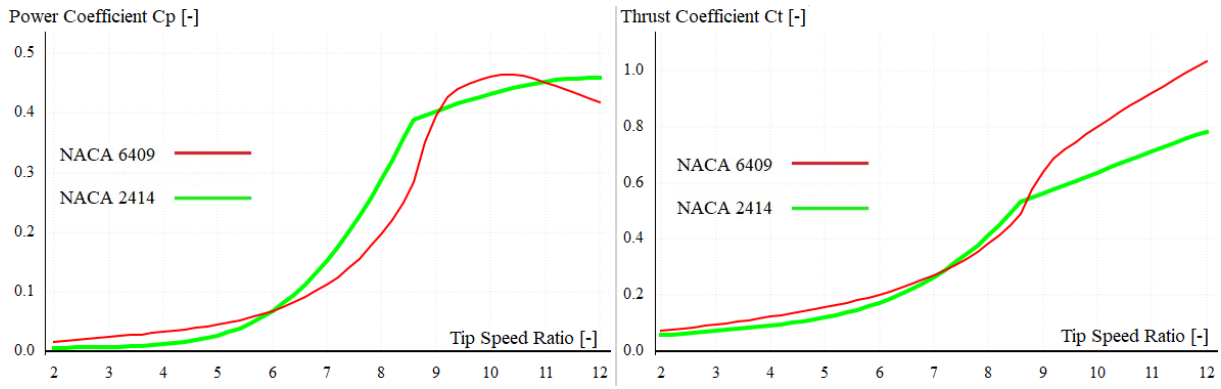

Figure 8. Comparative change graph of power (C_p) and thrust (C_t) coefficients of NACA 6409 and NACA 2414 airfoils according to tip velocity ratios

In terms of power coefficient, when Figure 8 and Figure 7 are analyzed together, it is naturally seen that the power coefficient and the amount of power obtained have the same graphical curve, and in terms of numerical data, NACA 2414 has a maximum power coefficient of 0.458 at 11.8 TSR and NACA 6409 has a maximum power coefficient of 0.465 at 10.4 TSR.

3. CONCLUSION

By using the Q-Blade software, with the blade element momentum (BEM) method, $1x10^6$ constant Re and $0\text{-}20^0$ angles of attack, keeping the air density and ambient conditions constant, the results obtained in this study, in which the design and comparative performance analysis of NACA 6409 and NACA 2414 series airfoils were carried out, are summarized as follows;

In terms of lift coefficient (C_l), it has been determined that the NACA 6409 airfoil has a more advantageous airfoil than NACA 2414 due to its high values in the $0^0\text{-}15^0$ angle of attack range. As the drag coefficient (C_d), it was observed that the drag coefficient of NACA 6409 increased rapidly in the $7^0\text{-}20^0$ angle of attack range, while NACA 2414 increased slowly with close values, and it was determined that NACA 2414 was more advantageous in terms of drag coefficient. In terms of the glide coefficient (C_l/C_d), which determines the efficiency of the blade profiles, it is

seen that both airfoils reach their peak values at 5^0 angle of attack, but the glide coefficient of NACA 6409 is 152,4 and NACA 2414 has a glide coefficient of 104.

It has been determined that NACA 6409 is more advantageous than NACA 2414 airfoil in the torque, torque, thrust and power coefficient analyzes made according to the tip speed ratios (TSR).

It has been determined that NACA 6409 compared to NACA 2414, as it has 5% less airfoil thickness ratio and 4% more camber ratio, has the advantages seen in Figures 6, 7 and 8.

Finally, when a comparative power generation analysis is made according to tip speed ratios at 10 m/sec wind speed with both airfoils with 3 blades and 2m blade length in the same ambient conditions, it is concluded that NACA 6409 produces more energy than NACA 2414.

NOMENCLATURE

NACA : National Advisory Committee for Aeronautics
BEM : Blade Element Momentum
TSR : Tip Speed Ratio
Re : Reynolds Number

ACKNOWLEDGMENT

Analyzes and comments made in this document belong to the authors. Article is not supported by any institution, company, and etc..

DECLARATION OF ETHICAL STANDARDS

The authors of the paper declare that nothing which is necessary for achieving the paper requires ethical committee and/or legal-special permissions.

CONTRIBUTION OF THE AUTHORS

Abdullah Tokul: Analysis, Acquisition of data, Interpretation of data, Writing - original draft.
Ünal Kurt: Conceptualization, Supervision, Writing - review & editing.

CONFLICT OF INTEREST

There is no conflict of interest in this study.

REFERENCES

[1] T.R. Energy and Natural Resources Ministry, Renewable Energy-Resources-Wind, Available: https://enerji.gov.tr/eigm-yenilenebilir-enerji-kaynaklar-ruzgar. Accessed: May. 13, 2023.

[2] Hansen MOL. Chapter 2 2-D Aerodynamics, Aerodynamics of Wind Turbines. London, Earthscan, 2008.

[3] Erişen A, Bakırcı M. NACA 0012 ve NACA 4412 kanat kesitlerinin yeniden tasarlanarak HAD ile analiz edilmesi. Journal of Engineering and Technology Sciences 2014; June: 50-82.

[4] Çil MA. Hava araçları ve rüzgâr türbinlerinde kullanılan farklı kanat profillerinin sayısal olarak incelenmesi. PhD Thesis, Erciyes University, 2022.

[5] Zahari MFB. A study of drag force on different type of airfoil in a subsonic wind tunnel. PhD Thesis, Pahang Malaysia University, 2013.

[6] Hossain MS, Raiyan MF, Akanda MNU, Jony HN. A comparative flow analysis of NACA 6409 and NACA 4412 aerofoil. International Journal of Research in Engineering and Technology 2014; 3(10): 342-350.

[7] Kumar R, Jhawar P, Kalraiya S. A CFD analysis of a wind turbine blade design at various angle of attack and low reynolds number. International Journal of Scientific Research & Engineering Trends 2016; 2(5): 126-132.

[8] Tarhan C, Yılmaz İ. Investigation of small wind turbine airfoils for Kayseri weather conditions. Fuels, Fire and Combustion in Engineering Journal 2016; 4(6): 42-43.

[9] Oliveira MS, Cândido LHA. Designing blades for horizontal-axis wind turbines applied to micro energy. International Journal of Advances in Engineering & Technology 2017; 10(1): 10-19.

[10] Sandanshiv SR, Chavan DUS. Aerodynamic performance study of wind turbine blade for variable airfoils. International Conference on Advances in Thermal Systems, Materials and Design Engineering 2017; Dec: 1-5.

[11] Muftah A. CFD modeling of airfoil of wind turbine under different effect of operating conditions. Sirte University Scientific Journal (Applied Sciences) 2019; 9(1): 27-43.

[12] Madhavan MN. Design and analysis of NACA 2414 aerofoil. International Journal of Scientific Research and Review 2019; 8(1): 161-168.

[13] Islam MR, Bashar LB, Saha DK, Rafi NS. Comparison and selection of airfoils for small wind turbine between NACA and NREL's S series airfoil families. International Journal of Research in Electrical, Electronics and Communication Engineering 2019; 4(2): 1-11.

[14] Kulshreshtha A, Gupta SK, Singhal P. FEM/CFD analysis of wings at different angle of attack. Materials Today: Proceedings 2020; March; 1638-1643.

[15] Mankotia P, Channi HK, Gupta S. Modeling and designing of small wind turbine blade. Journal Of Critical Reviews 2020; 7(19): 7276-7284.

[16] Hwas AM, Hatab AM. Effects of design parameters of wind turbine on airfoil coefficients using grey-based taguchi method. Journal of Multidisciplinary Engineering Science and Technology 2020; 7(12): 13103-13109.

[17] Gray A, Singh B, Singh S. Low Wind Speed Airfoil Design For Horizontal Axis Wind Turbine. Materials Today: Proceedings, 2021; 45; 3000-3004.

[18] Goyal S, Kulshreshtha A, Singh S. Selection of turbulence model for analysis of airfoil wing using CFD. International Research Journal of Engineering and Technology 2021; 8(3): 2608-2614.

[19] Solanki P. Computational fluid dynamics analysis of wind turbine blade at low reynolds number and various angle of attack. International Research Journal of Engineering and Technology 2021; 8(6): 4478-4485.

[20] Ahammed S. Optimization of floating horizontal axis wind turbine (fhawt) blades for aerodynamic performance measurement. Internatıonal Journal of Innovations in Engineering Research and Technology 2021; 8(6): 11-27.

[21] Widyalankara N, Jayawickrama NP, Ambegoda D, Velmanickam L. Optimum wind turbine design and analysis to harvest wind energy from fast-moving vehicles on highways. 3rd International Conference on Electrical Engineering 2021; Sep: 7-12.

[22] Marten D, Saverin J, Becker SP, Luna MRB. The Qblade Software. [Online]. Available: https://qblade.org/. Accessed: May. 18, 2023.

[23] Doğan K. Yatay eksenli rüzgâr türbin kanatlarının akışkan-yapı etkileşimi yönünden incelenmesi. PhD Thesis, Uludağ University, 2014.

[24] Marten D. QBlade: A modern tool for the aeroelastic simulation of wind turbines. PhD Thesis, Technical University of Berlin, 2020.

[25] Mahmuddin F. Rotor blade performance analysis with blade element momentum theory. Energy Procedia-The 8th International Conference on Applied Energy 2017; May: 1123 – 1129.

[26] Moriarty PJ, Hansen A. AeroDyn theory manual. National Renewable Energy Laboratory, Colorado, 2005.

[27] MIT Department of Aeronautics and Astronautics, Theory of Flight. Man-Vehicle Laboratory, [Online]. Available: https://web.mit.edu/16.00/www/aec/flight.html. Accessed: May. 18, 2023.

[28] Yükselen MA. Kanat profillerinin aerodinamiği. PhD Thesis, İstanbul Technical University, 2012.

[29] Cengiz Ç. Slatlı kanat profilinin etrafındaki düşük reynolds sayılı hava ve su akışlarının incelenmesi ve aerodinamik performans analizleri. PhD Thesis, Başkent University, 2010.

[30] King RM. Study of an adaptive mechanical turbulator for control of laminar separation bubbles. Raleigh North Carolina State University, 2001.

[31] Pitts WC, Nielsen JN, Kaattari GE. Lift and center of pressure of wing body tail combinations at subsonic, transonic, and supersonic speeds. National Advisory Committee for Aeronautics, California, 1957.

[32] Caboni M, Minisci E, Riccardi A. Aerodynamic design optimization of wind turbine airfoils under aleatory and epistemic uncertainty. Journal of Physics Conference Series, 2018; 1037(4): 1-10.

[33] Emniyetli G. Evsel elektrik ihtiyacının karşılanması için rüzgâr türbini tasarımı. PhD Thesis, Trakya University, 2007.

[34] Şenel MC, Koç E. Kanat tasarım parametrelerinin rüzgâr türbini aerodinamik performansına etkisi. V. Ulusal Havacılık ve Uzay Konferansı, Kayseri, 2014.

[35] Kaya K, Koç E. Yatay eksenli rüzgâr türbinlerinde kanat profil tasarımı ve üretim esasları. Mühendis ve Makine 2015; 56(670): 38-48.

[36] Gudmundsson S. The anatomy of the airfoil. General Aviation Aircraft Design: Applied Methods and Procedures 2014; 235-297.

[37] Amazon Services LLC Associates Program, Airfoil Tools. Amazon EU Associates Programme, [Online]. Available: http://airfoiltools.com/airfoil/naca4digit. Accessed: April. 24, 2023.

[38] Atılgan M, Altan BD, Atlıhan AB. Rüzgâr türbini uygulamaları. Chamber of Electrical Engineers Scientific Journal 2010; 1-7.

[39] Özden M. Rüzgâr türbini kanadında bütünleşik flap-girdap üretici mekanizmasının aerodinamik performansa etkisinin incelenmesi. PhD Thesis, Erciyes University, 2022; 6-7.

[40] Zhu C, Wang T, Wu J. Numerical investigation of passive vortex generators on a wind turbine airfoil undergoing pitch oscillations. Energies 2019; 12(654): 1-19.

[41] Widyawati G, Permatasari R. Effect of vortex generators on airfoil NACA 63_2-415 to aerodynamic characteristics using CFD. International Journal of Electrical, Energy and Power System Engineering (IJEEPSE) 2023; 6(1): 133-137.